

Dusty-gas model conservation law and approximate analytical solutions for H₂–H₂O transport in the SOFC anode support layer

Andrei Kulikovsky^{a)}
 Forschungszentrum Jülich GmbH
 Theory and Computation of Energy Materials (IET-3)
 Institute of Energy and Climate Research,
 D-52425 Jülich, Germany^{b)}

(Dated: 1 October 2024)

A complete Dusty-Gas Model for the H₂–H₂O mixture in the anode transport layer of the anode-supported SOFC is considered. An exact conservation law relating the total pressure and hydrogen molar fraction at any point inside the anode to their values in the anode channel is derived. Using this conservation law, approximate analytical solutions for the hydrogen molar fraction and total pressure in the anode transport layer are obtained. The solutions can be used to calculate concentration overpotential.

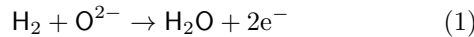
Keywords: Dusty-Gas Model, SOFC anode, two-component, analytical solution

I. INTRODUCTION

Anode-supported Solid Oxide Fuel Cells (SOFCs) employ thick, on the order of 1 mm, porous anode support layer (ASL). The ASL role is twofold: (i) it provides mechanical stability to the SOFC sandwich, and (ii) it serves as a transport layer for gases.

Mass transport through porous medium is a classic problem in chemical engineering¹. Huge surface area of pores dramatically increases the rate of surface-activated chemical or electrochemical reactions. In some devices, part of the porous domain is used for diffusive transport of gaseous or liquid components to/from the reaction zone. An important example is the anode-supported SOFC, where the porous ASL provides transport of hydrogen to and water from the thin reaction zone located near the electrolyte².

Schematic of the SOFC anode is shown in Figure 1. Hydrogen is supplied through the channel in the interconnect to the porous ASL, and finally to the anode active layer, where the electrochemical conversion of H₂ runs



The oxygen ions O²⁻ come to the active layer from the cathode side through the electrolyte. The product water is removed through the ASL to the channel / interconnect. The ASL thus supports two oppositely directed fluxes of hydrogen and water vapor.

It has been agreed that the most general description of multicomponent gaseous transport in porous media gives the Dusty-Gas Model (DGM)^{1,3,4}. The DGM equation for the molar fraction y_k of gaseous mixture k th component is

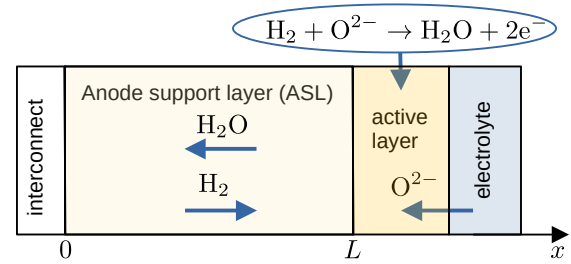


FIG. 1. Schematic of anode-supported SOFC anode. The sketch is strongly not to scale: the active layer thickness is two orders of magnitude smaller than the ASL thickness.

(Zhu and Kee⁵):

$$\sum_{i \neq k} \frac{y_i N_k - y_k N_i}{D_{ik}} + \frac{N_k}{D_{K,k}} = -\frac{1}{RT} \left(\frac{\partial(y_k p)}{\partial x} + \frac{y_k}{D_{K,k}} \frac{p B_0}{\mu} \frac{\partial p}{\partial x} \right) \quad (2)$$

or, equivalently,

$$\sum_{i \neq k} \frac{y_i N_k - y_k N_i}{D_{ik}} + \frac{N_k}{D_{K,k}} = -\frac{p}{RT} \frac{\partial y_k}{\partial x} - \frac{1}{RT} \left(y_k + \frac{y_k}{D_{K,k}} \frac{p B_0}{\mu} \right) \frac{\partial p}{\partial x} \quad (3)$$

Here N_k is the molar flux, p the pressure, $D_{i,k}$ the effective binary molecular diffusion coefficient, $D_{K,k}$ the effective Knudsen diffusion coefficient, B_0 the hydraulic permeability of the porous media, m the mixture viscosity. The DGM takes into account the inter-diffusion Stefan-Maxwell fluxes (the first term on the left side), the Knudsen diffusion in smaller pores (the second term on the left side), and the flux due to the pressure gradient (the last term in Eq.(3)).

The term with pressure gradient introduces quite significant complexity to the analysis and in many works this

^{a)}ECS member; Electronic mail: A.Kulikovsky@fz-juelich.de

^{b)}Also at: Lomonosov Moscow State University, Research Computing Center, 119991 Moscow, Russia

term has been neglected^{6–11}. This simplifies the DGM to the Stefan–Maxwell–Knudsen Model (SMKM):

$$\sum_{i \neq k} \frac{y_i N_k - y_k N_i}{D_{ik}} + \frac{N_k}{D_{K,k}} = -\frac{p}{RT} \frac{\partial y_k}{\partial x} \quad (4)$$

An exact consequence of SMKM is the Graham's law¹²

$$\sum_k N_k \sqrt{M_k} = 0 \quad (5)$$

which is obtained by summing Eq.(4) over k , taking into account that $\sum_k y_k = 1$ and $D_{K,k} \sim 1/\sqrt{M_k}$. Here M_k is the molecular weight of the k th component. However, in SOFC anode, water and hydrogen fluxes are related by stoichiometry requirement $N_w = -N_h$, which follows from Eq.(1). This relation is provided by the pressure gradient, which is missing in SMKM.

Several works have demonstrated importance of the pressure gradient term^{13–15} (note a typo in Eq.(35a) of Ref.¹⁴). Fu et al.⁴ have shown that the inequality of hydrogen and water Knudsen diffusion coefficients generates pressure gradient in the porous media. Indeed, if in a two–component system $M_1 = M_2$, the Graham's law, Eq.(5), reduces to the SOFC anode stoichiometry relation $N_1 + N_2 = 0$. Thus, if the molecular weights of water M_w and hydrogen M_h were equal, the SMKM would have been equivalent to the DGM. In fact, however, $\sqrt{M_w/M_h} = 3$, which makes the things more complicated. Bertei and Nicoletta¹⁵ discussed this and several other inconsistencies in models for porous electrode.

In this work, a complete two–component DGM for H₂–H₂O transport in the SOFC ASL is considered. An exact conservation law is derived relating the total pressure and hydrogen concentration at any point inside the anode to their values in the channel. Further, approximate analytical solutions for the DGM equations are constructed using the conservation law. Comparison with numerical results shows good accuracy of the analytical shapes.

II. MODEL

A. Two–component DGM equations

Equation for the hydrogen molar fraction $y \equiv y_h$ in the two–component mixture of H₂–H₂O is obtained from Eq.(2) taking into account that $y_w = 1 - y$ and $N_w = -N_h$:

$$\frac{\partial(y p)}{\partial x} + \frac{y p B_0}{D_{K,h} \mu} \frac{\partial p}{\partial x} = -\frac{RT}{D_{K,h}} (1 + K) N_h \quad (6)$$

where the subscripts w and h denote water and hydrogen. Equation for the total pressure is obtained by summing up Eqs.(3). Taking into account that the Stefan–Maxwell terms cancel out, $\sum_k y_k = 1$, and $\sum_k y_k / D_{K,k} =$

$(Q + y(1 - Q))/D_{K,h}$, we get

$$\left(1 + (Q + y(1 - Q)) \frac{p B_0}{D_{K,h} \mu}\right) \frac{\partial p}{\partial x} = -\frac{RT}{D_{K,h}} (1 - Q) N_h \quad (7)$$

Here,

$$K = \frac{D_{K,h}}{D_m}, \quad Q = \frac{D_{K,h}}{D_{K,w}} = \sqrt{\frac{M_w}{M_h}} = 3. \quad (8)$$

Eq.(6) suggests a suitable characteristic scale for pressure. Introducing dimensionless variables

$$\tilde{x} = \frac{x}{L}, \quad \tilde{p} = \frac{p}{p_*}, \quad p_* = \frac{\mu D_{K,h}}{B_0} \quad (9)$$

and setting $Q = 3$, from Eqs.(6), (7) we find

$$\frac{\partial(y \tilde{p})}{\partial \tilde{x}} + y \tilde{p} \frac{\partial \tilde{p}}{\partial \tilde{x}} = -(1 + K) \tilde{N}_h \quad (10)$$

$$(1 + \tilde{p}(3 - 2y)) \frac{\partial \tilde{p}}{\partial \tilde{x}} = 2 \tilde{N}_h \quad (11)$$

where the dimensionless hydrogen molar flux is

$$\tilde{N}_h = \frac{N_h}{N_*}, \quad N_* = \frac{\mu D_{K,h}^2}{RT L B_0} \quad (12)$$

B. Mass transport equations

Hydrogen mass conservation prescribes that

$$\frac{\partial \tilde{N}_h}{\partial \tilde{x}} = 0. \quad (13)$$

Differentiating Eqs.(10), (11) over \tilde{x} , we thus get

$$\frac{\partial}{\partial \tilde{x}} \left(\frac{\partial(y \tilde{p})}{\partial \tilde{x}} + y \tilde{p} \frac{\partial \tilde{p}}{\partial \tilde{x}} \right) = 0 \quad (14)$$

$$\frac{\partial}{\partial \tilde{x}} \left((1 + \tilde{p}(3 - 2y)) \frac{\partial \tilde{p}}{\partial \tilde{x}} \right) = 0 \quad (15)$$

It is worth noting that the system of Eqs.(14), (15) does not contain parameters.

C. Boundary (initial) conditions

At the channel/ASL interface $y = y_c$, $\tilde{p} = \tilde{p}_c$. where the subscript c marks the values in the channel. The reaction stoichiometry prescribes that the hydrogen flux $N_h = J/(2F)$ and from Eq.(10) we, thus, get

$$\tilde{p}_c \frac{\partial y}{\partial \tilde{x}} \Big|_{\tilde{x}=0} = -y_c (1 + \tilde{p}_c) \frac{\partial \tilde{p}}{\partial \tilde{x}} \Big|_{\tilde{x}=0} - (1 + K) \tilde{J} \quad (16)$$

where

$$\tilde{J} = \frac{J}{J_*}, \quad J_* = 2FN_* = \frac{2F\mu D_{K,h}^2}{RTL B_0} \quad (17)$$

Quite similarly, from Eq.(11) we find

$$\left. \frac{\partial \tilde{p}}{\partial \tilde{x}} \right|_{\tilde{x}=0} = \frac{2\tilde{J}}{1 + \tilde{p}_c(3 - 2y_c)} \equiv W \quad (18)$$

III. CONSERVATION LAW AND APPROXIMATE ANALYTICAL SOLUTION

Since $\tilde{N}_h = \tilde{J}$, Eqs.(10), (11) can be written as

$$\frac{\partial(y\tilde{p})}{\partial \tilde{x}} + y\tilde{p} \frac{\partial \tilde{p}}{\partial \tilde{x}} = -(1 + K)\tilde{J} \quad (19)$$

$$(1 + \tilde{p}(3 - 2y)) \frac{\partial \tilde{p}}{\partial \tilde{x}} = 2\tilde{J} \quad (20)$$

With the constant right sides, Eqs.(19), (20) automatically satisfy the mass transport Eqs.(14), (15). Multiplying Eq.(19) by 2 and summing with Eq.(20), we get

$$2 \frac{\partial(y\tilde{p})}{\partial \tilde{x}} + (1 + 3\tilde{p}) \frac{\partial \tilde{p}}{\partial \tilde{x}} = -2K\tilde{J} \quad (21)$$

Rewriting this equation as

$$2 \frac{\partial(y\tilde{p})}{\partial \tilde{x}} + \frac{\partial \tilde{p}}{\partial \tilde{x}} + \frac{3}{2} \frac{\partial(\tilde{p}^2)}{\partial \tilde{x}} = -2K\tilde{J} \quad (22)$$

we see that it can be integrated from 0 to \tilde{x} yielding a conservation law:

$$2(y\tilde{p} - y_c\tilde{p}_c) + (\tilde{p} - \tilde{p}_c) + \frac{3}{2}(\tilde{p}^2 - \tilde{p}_c^2) = -2K\tilde{J}\tilde{x} \quad (23)$$

Eq.(23) can be derived for the two-component system CO-CO₂. Eq.(19) does not change, while Eq.(7) in the dimensionless form reads

$$(1 + \tilde{p}(Q - y(Q - 1))) \frac{\partial \tilde{p}}{\partial \tilde{x}} = -(1 - Q)\tilde{J} \quad (24)$$

Multiplying Eq.(19) by $(Q - 1)$ and summing with Eq.(24) we get

$$(Q - 1) \frac{\partial(y\tilde{p})}{\partial \tilde{x}} + (1 + Q\tilde{p}) \frac{\partial \tilde{p}}{\partial \tilde{x}} = -(Q - 1)K\tilde{J} \quad (25)$$

Integrating Eq.(25) we find

$$(Q - 1)(y\tilde{p} - y_c\tilde{p}_c) + (\tilde{p} - \tilde{p}_c) + \frac{Q}{2}(\tilde{p}^2 - \tilde{p}_c^2) = -(Q - 1)K\tilde{J}\tilde{x} \quad (26)$$

where $Q = \sqrt{28/44}$ for the CO-CO₂ pair.

A simple analytical formula for the hydrogen molar fraction through the ASL depth can be obtained from the conservation law as follows. The variation of product $\tilde{p}y_k$ along

Cell temperature, K	T	273 + 800
Pressure in the channel, Pa	p_c	10^5
Current density, A m ⁻²	J	10^4
Anode thickness, m	L	10^{-3}
Mean pore diameter, m	d	10^{-6}
Porosity/tortuosity ratio	λ	0.033, Ref. ⁷
Hydrogen viscosity at 800 °C, Pa s	μ	$2 \cdot 10^{-5}$
Free binary molecular diff. m ² s ⁻¹	D_m^{free}	$8.154 \cdot 10^{-4}$, Ref. ⁷
Anode gas composition		85%H ₂ + 15%H ₂ O

TABLE I. Cell parameters used in calculations.

\tilde{x} is not large and hence the term with pressure gradient in the DGM, Eq.(2), is close to the D'Arcy law describing flow in a pipe. We, therefore, may expect that the deviation of pressure gradient from a constant value is small. From Eq.(18) it follows that a reasonably good approximation for $\tilde{p}(\tilde{x})$ is a linear function

$$\tilde{p} \simeq \tilde{p}_c + W\tilde{x} \quad (27)$$

Solving Eq.(23) for y and substituting \tilde{p} , Eq.(27), into the resulting equation, we get

$$y = \frac{1}{\tilde{p}_c + W\tilde{x}} \left(y_c\tilde{p}_c - \frac{3}{4}W^2\tilde{x}^2 - \left(\frac{(3\tilde{p}_c + 1)}{2}W + K\tilde{J} \right) \tilde{x} \right) \quad (28)$$

At $\tilde{x} = 1$, Eqs.(28), (27) give the hydrogen molar concentration $c_a = p_*\tilde{p}_a y_a / (RT)$ at the active layer:

$$c_a = \frac{p_*}{RT} \left(y_c\tilde{p}_c - \frac{3}{4}W^2 - \left(\frac{(3\tilde{p}_c + 1)}{2}W + K\tilde{J} \right) \right), \quad \text{mol m}^{-3} \quad (29)$$

Similar results for CO-CO₂ mixture can be easily derived from Eqs.(26), (27).

IV. RESULTS AND DISCUSSION

Parameters used in the calculations below are collected in Table I. The transport coefficients were calculated as

$$\begin{aligned} B_0 &= \frac{\lambda d^2}{32}, \quad \text{Ref.}^{15} \\ D_{K,h} &= \frac{\lambda d}{3} \sqrt{\frac{8RT}{\pi M_h}} \\ D_m &= \lambda D_m^{free} \end{aligned} \quad (30)$$

where λ is the porosity/tortuosity ratio, d is the mean pore diameter (Table I).

Setting in Eq.(23) $\tilde{p} = \tilde{p}_c$ we get the linear hydrogen molar fraction shape (Fick's law) corresponding to zero pressure gradient in the ASL:

$$y = y_c - \frac{RTLJ}{2FD_m p_c} \frac{x}{L} \quad (31)$$

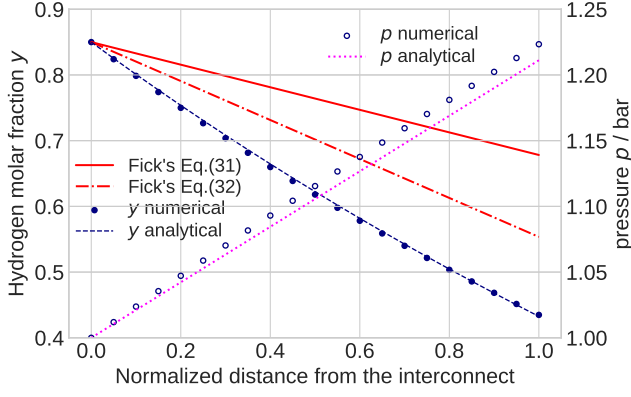


FIG. 2. The shapes of hydrogen molar fraction through the one-mm thick Ni-YSZ cermet anode calculated using the Fick's law Eq.(31) (solid line), Eq.(32) (dash-dotted line), from the numerical solution to the DGM model Eqs.(19), (20) (solid points), and using the analytical solution Eq.(28) (dashed line). Open circles show numerical pressure from the DGM model (right axis), dotted line is the approximate linear formula for $p(\tilde{x})$, Eq.(27).

In literature, another version of the Fick's law, which follows from the SMKM has been used^{16,17}:

$$y = y_c - \frac{RTLJ}{2Fp_c} \left(\frac{1}{D_m} + \frac{1}{D_{K,h}} \right) \frac{x}{L} \quad (32)$$

Figure 2 shows the linear shapes of y from the Fick's law, Eq.(31) and Eq.(32), the exact numerical solution to the problem (19), (20), and the approximate analytical Eq.(28). The numerical and analytical, Eq.(27), shapes of pressure are also shown.

Both Fick's equations, Eqs.(31),(32) quite significantly overestimate the exact hydrogen molar fraction (Figure 2). Physically, Knudsen diffusion leads to formation of the positive pressure gradient (Figure 2), which retards hydrogen diffusion toward the active (reaction) zone, while Fick's equations ignore this effect. In addition, the Fick's law is used in literature together with the constant pressure assumption, hence the error in calculated hydrogen molar concentration $c = yp/(RT)$ is even larger than the error in y itself demonstrated in Figure 2.

The analytical shape of hydrogen molar fraction, Eq.(28), approximates the numerical result very well (Figure 2). The linear shape of pressure, Eq.(27), is somewhat less accurate, though the maximal error at the ASL/active layer interface is about 1% only (Figure 2). It is worth noting that for lower currents, the agreement of analytical and numerical pressure shapes is better. Eq.(29) could, thus, be recommended for calculation of concentration polarization in SOFC anode instead of a widely used Fick's law.

The Fick's law, Eq.(31) results from the conservation law under the condition $\partial \tilde{p} / \partial \tilde{x} = 0$ and it shows that y is independent of the Knudsen diffusivity. Therefore, in the case of H_2 - H_2O mixture, the Stefan-Maxwell-Knudsen model,

Eq.(4), and in particular Eq.(32), is contradictory. Indeed, from Eq.(31) it follows that to neglect pressure gradient in Eq.(3), both $\partial p / \partial x$ and Knudsen $N_k / D_{K,k}$ terms must be omitted, rather than $\partial p / \partial x$ term alone.

The conservation law, Eq.(23), provides several opportunities. Setting in Eq.(23) $\tilde{x} = 1$, we get a relation between parameters in the channel and at the ASL/active layer interface:

$$2(y_a \tilde{p}_a - y_c \tilde{p}_c) + (\tilde{p}_a - \tilde{p}_c) + \frac{3}{2} (\tilde{p}_a^2 - \tilde{p}_c^2) = -2K\tilde{J} \quad (33)$$

where the subscript a marks the values at $\tilde{x} = 1$. In the dimension form Eq.(33) reads

$$2(y_a p_a - y_c p_c) + p_a - p_c + \frac{3}{2} (p_a^2 - p_c^2) \frac{B_0}{\mu D_{K,h}} = -\frac{RTLJ}{FD_m} \quad (34)$$

From practical perspective, measuring pressure p_a one can calculate hydrogen molar fraction y_a using Eq.(34). Another useful options arise in the case of limiting current density: setting in Eq.(34) $y_a = 0$, we get the relation between y_c , p_c , p_a and the system transport parameters:

$$-2y_c p_c + p_a - p_c + \frac{3}{2} (p_a^2 - p_c^2) \frac{B_0}{\mu D_{K,h}} = -\frac{RTLJ}{FD_m} \quad (35)$$

Eq.(35) allows for direct calculation of pressure p_a at the active layer. On the other hand, by measuring p_a in this regime, the relation between $D_{K,h}$, B_0 and D_m results, hence any one of this three transport parameters can be estimated provided that the other two are known. Measuring pressure inside the porous sandwich at high temperature is a challenging task¹⁸. However, in the future it could be feasible.

V. CONCLUSIONS

An exact first integral (the conservation law) of the Dusty-Gas Model for the two-component mixture in SOFC anode support layer is derived. Based on this result, approximate analytical solution for the hydrogen molar fraction and total pressure shapes in the ASL are obtained. Comparison with the numerical solution of the full system of DGM equations shows a good quality of the approximate solutions. A simple formula for the hydrogen molar concentration at the ASL/active layer interface could be employed for calculation of concentration overpotential instead of the widely used Fick's law.

- ¹E. A. Mason and A. P. Malinauskas. *Transport in Porous Media: The Dusty Gas Model*. Elsevier, New-York, 1983.
- ²A. McEvoy. Anodes. In S. C. Singhal and K. Kendall, editors, *High Temperature Solid Oxide Fuel Cells. Fundamentals, Design and Applications*, pages 149–172. Elsevier, Amsterdam, 2003.
- ³H. Zhu, R. J. Kee, V. M. Janardhanan, O. Deutschmann, and D. Goodwin. Modeling elementary heterogeneous chemistry and electrochemistry in solid-oxide fuel cells. *J. Electrochem. Soc.*, 152:A2427–A2440, 2005. doi:10.1149/1.2116607.
- ⁴Y. Fu, Y. Jiang, S. Poizeau, A. Dutta, A. Mohanram, J. D. Pietras, and M. Z. Bazant. Multicomponent gas diffusion in porous electrodes. *J. Electrochem. Soc.*, 162:F613–F621, 2015. doi:10.1149/2.0911506jes.
- ⁵H. Zhu and R. J. Kee. Modeling distributed charge–transfer processes in SOFC membrane–electrode assemblies. *J. Electrochem. Soc.*, 155:B715–B729, 2008.
- ⁶W. Lehnert, J. Meusinger, and R. Thom. Modeling of gas transport phenomena in SOFC anodes. *J. Power Sources*, 87:57–63, 2000.
- ⁷C. Bao and N. Cai. An approximate analytical solution of transport model in electrodes for anode–supported solid oxide fuel cells. *AIChE J.*, 53:2968–2979, 2007. doi:10.1002/aic.11297.
- ⁸Y. Shi, N. Cai, C. Li, C. Bao, E. Croiset, J. Qian, Q. Hu, and S. Wang. Simulation of electrochemical impedance spectra of solid oxide fuel cells using transient physical models. *J. Electrochem. Soc.*, 155:B270–B280, 2008. doi:10.1149/1.2825146.
- ⁹F. N. Cayan, S. R. Pakalapati, F. Elizalde-Blancas, and I. Celik. On modeling multi-component diffusion inside the porous anode of solid oxide fuel cells using Fick’s model. *J. Power Sources*, 192:467–474, 2009. doi:10.1016/j.jpowsour.2009.03.026.
- ¹⁰A. Häffel, J. Joos, M. Ender, A. Weber, and E. Ivers-Tiffée. Time-dependent 3D impedance model of mixed-conducting solid oxide fuel cell cathodes. *J. Electrochem. Soc.*, 160:F867–F876, 2013. doi:10.1149/2.093308jes.
- ¹¹F. Yang, J. Gu, L. Ye, Z. Zhang, G. Rao, Y. Liang, K. Wen, J. Zhao, J. B. Goodenough, and W. He. Justifying the significance of Knudsen diffusion in solid oxide fuel cells. *Energy*, 95:242–246, 2016. doi:10.1016/j.energy.2015.12.022.
- ¹²R. Krishna and J. A. Wesselingh. The Maxwell–Stefan approach to mass transfer. *Chem. Eng. Sci.*, 52:861–911, 1997. doi:10.1016/S0009-2509(96)00458-7.
- ¹³H. Zhu, R. J. Kee, V. M. Janardhanan, O. Deutschmann, and D. Goodwin. Modeling electrochemical impedance spectra in SOFC button cells with internal methane reforming. *J. Electrochem. Soc.*, 152:A2427–A2440, 2005.
- ¹⁴I. K. Kookos. On the diffusion in porous electrodes of SOFCs. *Chem. Engineer. Sci.*, 69:571–577, 2012. doi:10.1016/j.ces.2011.11.013.
- ¹⁵A. Bertei and C. Nicoletta. Common inconsistencies in modeling gas transport in porous electrodes: The dusty-gas model and the Fick law. *J. Power Sources*, 279:133–137, 2015. doi:10.1016/j.jpowsour.2015.01.007.
- ¹⁶R. Suwanwarangkul, E. Croiset, M. W. Fowler, P. L. Douglas, E. Entchev, and M. A. Douglas. Performance comparison of Fick’s, dusty–gas and Stefan–Maxwell models to predict the concentration overpotential of a SOFC anode. *J. Power Sources*, 122:9–18, 2003. doi:10.1016/S0378-7753(02)00724-3.
- ¹⁷J. Ma, M. Yan, Y. Zhang, and S. Quin. Analysis of mass transport in solid oxide fuel cells using a thermodynamically consistent model. *Int. J. Energy Res.*, 46:6487–6497, 2022. doi:10.1002/er.7586.
- ¹⁸M. Nagata and H. Iwahara. The measurement of water vapour pressure in an SOFC anode during discharge. *J. Appl. Electrochem.*, 23:275–278, 1993. doi:10.1007/BF00296681.

NOMENCLATURE

\sim	Marks dimensionless variables
B_0	Hydraulic permeability, m^2 , Eq.(30)
d	Mean pore diameter, m
c	Hydrogen molar concentration, mol m^{-3}
c_a	Hydrogen molar concentration at the active layer, mol m^{-3}
$D_{h,w}$	Effective binary molecular diffusion coefficient in H_2 – H_2O mixture, $\text{m}^2 \text{s}^{-1}$
$D_{K,h}$	Effective Knudsen diffusion coefficient of hydrogen, $\text{m}^2 \text{s}^{-1}$
$D_{K,w}$	Effective Knudsen diffusion coefficient of water, $\text{m}^2 \text{s}^{-1}$
F	Faraday constant, C mol^{-1}
J	Cell current density, A m^{-2}
K	$K = D_K/D_m$
L	Anode support layer thickness, m
M_i	Molecular weight of the i th component, kg mol^{-1}
N_i	Molar flux of the i th component, $\text{mol m}^{-2} \text{s}^{-1}$
p	Pressure, Pa
p^*	Characteristic pressure, Pa, Eq.(9)
q	Dimensionless parameter, $0 \leq q \leq 1$
R	Gas constant, $\text{J K}^{-1} \text{mol}^{-1}$
T	Cell temperature, K
W	$\equiv \partial \tilde{p} / \partial \tilde{x} _{\tilde{x}=0}$, Eq.(18)
x	Coordinate through the anode support layer, m
y	Molar fraction of hydrogen
y_i	Molar fraction of the i th component

Subscripts:

*	Characteristic value
a	ASL/active layer interface
c	Channel/ASL interface
h	Hydrogen
K	Knudsen diffusion
m	molecular diffusion
w	Water

Greek:

λ	Porosity/tortuosity ratio
μ	Dynamic viscosity, Pa s